Fine structure of the Ca 2p x-ray-absorption edge for bulk compounds, surfaces, and interfaces

F. J. Himpsel, U. O. Karlsson,* A. B. McLean,† and L. J. Terminello
IBM Research Division, Thomas J. Watson Research Center, P.O. Box 218, Yorktown Heights, New York 10598

F. M. F. de Groot, M. Abbate, and J. C. Fuggle
Research Institute for Materials, University of Nijmegen, Toernooiveld, 6525 ED Nijmegen, The Netherlands

J. A. Yarmoff
Department of Physics, University of California, Riverside, California 92521

B. T. Thole and G. A. Sawatzky
Materials Science Centre, University of Groningen, Nijenborgh 18, Paddepoel, 9747 AG Groningen, The Netherlands
(Received 15 October 1990)

The fine structure of the Ca 2p soft-x-ray-absorption edge is studied for a variety of bulk compounds (Ca metal, $CaSi_2$, CaO, and CaF_2), for surfaces and interfaces [CaF_2(111), BaF_2 on CaF_2(111), Ca and CaF_2 on Si(111)], and for defects (*F* centers in CaF_2). The observed multiplet structure is explained by atomic calculations in a crystal field [cubic O_h for the bulk and threefold C_{3v} for the (111) surfaces and interfaces]. While the bulk spectra are isotropic, the surface and interface spectra exhibit a pronounced polarization dependence, which is borne out by the calculations. This effect can be used to become surface and/or interface selective via polarization-modulation experiments, even for buried interfaces. A change in valence from Ca^{2+} to Ca^{1+} causes a downwards energy shift and extra multiplet lines according to the calculation. The energy shift is observed for *F* centers at the CaF_2 surface and for the CaF_2/Si(111) interface.

I. INTRODUCTION

The fine structure of x-ray-absorption edges is a useful probe for the structural environment of atoms and their chemical state.[1-3] For example, there is a relationship between the fine structure of the absorption edge and the oxidation state, or valence, of the absorbing atom. A program correlating the multiplet structure of an absorption edge with the valence has been successfully carried out for the rare earths.[2,3] Similar attempts are beginning to take hold for transition metals.[4-15] The task is more difficult for the latter, since the atomic multiplet splittings are smaller. Consequently, they are affected by the crystal field and broadened by band formation. Despite these difficulties, it has been possible in some cases to identify the valence and even the spin alignment[11] from the multiplet structure. The knowledge of the valence is important for materials as diverse as high-temperature superconductors[16-19] and metalorganic compounds[10] (phthalocyanines, hemoglobin, chlorophpyll).

A second avenue is just opening up, i.e., the spectroscopy of buried interfaces. The main difficulty is to penetrate the overlayer, and still be sensitive to a monolayer at the interface. It has been pointed out that the core level and Auger shifts at the interface can be used to become interface selective.[20] In addition, the lower symmetry of the interface causes anisotropy, which distinguishes interface transitions from bulk transitions by their polarization dependence. The same arguments apply to surfaces Polarization-modulation spectroscopy at core-level absorption edges could become a viable tool when using the high brilliance of undulator-based synchrotron radiation sources. This method would pick out the interface (surface) contribution in a clean way, even for buried interfaces, where very few techniques are available.

The Ca 2p edge is a prime candidate for testing the feasibility of these concepts. The fine structure is very sharp, since it is mainly due to localized Ca 2p-to-3d transitions.[21,22] Therefore an atomic picture is a good starting point. Ca has been the subject of widespread interest, ranging from biology to semiconductor physics. For example, microscopy of Ca-containing bone tissue has been performed with x rays at the Ca 2p absorption edge.[23] The CaF_2/Si(11) interface has been studied extensively[20,24-30] because of its high structural quality, and interface-related structures have been observed at the Ca 2p absorption edge.[20,25,27] Here we aim at an in-depth understanding of the fine structure for various model compounds, surfaces, interfaces, and defects. For this purpose we correlate the experimental spectra with calculations of the atomic multiplet structure that include the effect of the crystal field, valence changes, and the lowering of the symmetry at surfaces and interfaces.

II. EXPERIMENT

The experiments were carried out with a 10-m toroidal grating monochromator[31] (TGM), combined with a display spectrometer[32] at the National Synchrotron Light Source at Brookhaven. Core-level absorption was measured by detecting Auger electrons, which are proportional to the number of core holes created in the absorp-

tion process. In some instances we also collected secondary electrons and photodesorbed positive ions. The latter were used to obtain a signal from the immediate surface region. Auger and secondary electrons gave similar results,[33] as long as the energy detection window for Auger electrons was kept sufficiently wide (9 eV in our case) to cover the main part of the Auger multiplet structure.[20,27,34–36] By selecting portions of the Auger spectrum it was possible to enhance certain members of the absorption edge multiplet (see Fig. 4). Similarly, the energy shift between bulk and interface Auger peaks[20,27] could be used to selectively enhance bulk or interface features, depending on the placement of the energy window. It should be noted that the cross section in the main Ca $2p$ absorption lines of CaF_2 is so large that saturation effects are encountered, particularly when the incident light is close to grazing. In this case the escape depth of the Auger (secondary) electrons becomes larger than the absorption depth of the light, and all core holes contribute to the electron yield, independent of the absorption coefficient. As noted early on,[37] this violates the principal premise of absorption spectroscopy in the partial-yield mode, which requires that the electron escape depth is small compared to the photon absorption depth. The polarization was varied from s polarization, with light incident normal to the sample surface, to p polarization with light incident about 60° from normal.

The samples were prepared as follows: CaF_2 was grown epitaxially[20,24–30] on a clean Si(111)7×7 surface at about 700 °C, with postanneals in the 800 °C–850 °C range, depending on thickness. Cleaved single crystals were also used, but they gave broader structures, since heating was required to avoid charging. CaO single crystals[38] were cleaved and heated. Ca was evaporated. $CaSi_2$ was prepared by evaporating Ca onto Si and annealing.[31] For thin epitaxial CaF_2 films on Si(111) the thickness could be monitored by observing the Ca $2p$ and Ca $3d$ core level intensities of the shifted interface peak.[24–28] It should be noted that the ionic Ca compounds are very sensitive to radiation damage[40–42] (see also Sec. VI). However, the dose to collect an absorption spectrum with the efficient display spectrometer[32] was about 10^3 times less than that required for radiation damage to occur.

III. CALCULATION METHOD

The Ca $2p$ electron has dipole-allowed transitions into s- and d-like final states, the lowest being Ca $4s$ and Ca $3d$. The $3d$ channel is by far stronger than the other channels since the $3d$ wave functions collapse in the presence of the Ca $2p$ core hole, and thus dramatically increase their overlap with the Ca $2p$.[21,22] This makes the problem of calculating the Ca $2p$ absorption edge amenable to an atomic multiplet approach, i.e., the calculation of the Ca^{2+} $2p^6 3d^0$-to-$2p^5 3d^1$ dipole transition. Thereby one starts from the premise that the interaction of the core hole with the excited electron dominates over the interactions with neighboring atoms. The local environment in the solid is then taken into account as the adaptation of the spherically symmetric, atomic field to the crystal symmetry. The first step is the inclusion of a cubic (octahedral) crystal field, representing the O_h symmetry in the bulk Ca compounds studied here. It is represented by a single parameter X^{400}. Then the symmetry is reduced to C_{3v}, representing the threefold $CaF_2(111)$ surface or interface. In this case one has two extra parameters,[43] i.e., $X^{4\bar{1}0}$ and $X^{2\bar{1}0}$. The total crystal-field Hamiltonian in C_{3v} symmetry is

$$H_{\mathrm{CF}} = X^{400}U^{400} + X^{4\bar{1}0}U^{4\bar{1}0} + X^{2\bar{1}0}U^{2\bar{1}0} .$$

The U's are unitary transformations, which relate to scaling factors of 0.304, 0.530, and 0.358, respectively. The $X^{400}U^{400}$ term, also denoted by $10Dq$, splits the d orbitals into a triply degenerate t_{2g} (Γ'_{25}) and a double degenerate e_g (Γ_{12}) manifold, excluding spin degeneracy. The $X^{4\bar{1}0}$ and $X^{2\bar{1}0}$ terms split the t_{2g} manifold into a doublet (Λ_3) and a singlet (Λ_1). The e_g manifold turns into a Λ_3 doublet in the C_{3v} symmetry, and mixes with the Λ_3 doublet derived from the t_{2g} manifold. The crystal-field parameters are fitted to the experimental multiplet structure. Since the $X^{4\bar{1}0}$ and $X^{2\bar{1}0}$ terms do not modify the average cubic crystal-field splitting, one can use the bulk X^{400} term as a starting point for calculating a surface multiplet. Details concerning the group theory and the calculation methods can be found in the book by Butler[43] and in Ref. 44.

IV. BULK COMPOUNDS

X-ray absorption spectra of Ca^{2+} are shown on the bottom of Fig. 1 for octahedral, sixfold coordination in CaO and for cubic, eightfold coordination in CaF_2. They are reproduced by our multiplet calculations using crystal-field parameters $10Dq$ of +1.2 and −0.75 eV, respectively (Fig. 1, top). The theoretical CaO spectrum consists of seven allowed transitions, which are broadened by a combination of a Gaussian and a Lorentzian to simulate broadening mechanisms originating from band dispersion, vibrations, and (autoionization) decay. These broadening mechanisms are found to result in different values for every of the four main peaks.[12] As the main interactions are the core-hole spin-orbit splitting and the crystal field, the four main peaks can be loosely assigned as $2p_{3/2}$-t_{2g}, $2p_{3/2}$-e_g, $2p_{1/2}$-t_{2g}, $2p_{1/2}$-e_g, in order of increasing energy. The small leading peaks originate from the mixing of states due to the multipole interaction of the core hole with the valence electron, combined with the $3d$ spin-orbit splitting. The absolute energy scale is off by about 2 eV. This originates mainly from the neglect of screening. The interpretation of the CaF_2 spectrum is similar, but due to the eightfold surrounding one has a negative $10Dq$, and the order of the t_{2g} and e_g orbitals is reversed. The intensity of the e_g peaks is low, which prohibits a simple assignment of the $2p_{3/2}$ (L_3) part.

The Ca $2p$ absorption spectra of Ca in metallic environments, such as Ca metal and $CaSi_2$, show two broad peaks with a weak, sharper structure at the onset (Fig. 2, bottom). Note that the core-level binding energies relative to the Fermi level (vertical bars in Fig. 2) coincide with the onset of the absorption. This triplet structure is

similar to a broadened version of the calculated atomic multiplet (Fig. 2, top), which agrees well with the atomic spectrum of Ca reported in the literature.[21] This indicates a weak crystal field, which is consistent with the more homogeneous, jelliumlike charge distribution in a metal, as opposed to the strong point charges in an ionic insulator. Though it is possible to simulate the spectra with the multiplet approach, the information that can be gained is limited because of the large broadenings and possible modifications due to band dispersion effects. However, we note that the agreement that can be reached from this approach is at least similar to the results for Ca obtained by Zaanen *et al.*[9]

We note that the spectrum of a submonolayer of Ca on Si(111) in Fig. 2 also bears clear resemblance to the atomic spectrum, with less broadening than in Ca metal and $CaSi_2$. This indicates that the Ca atom is bonded weakly to the Si(111) surface, in other words, that the bonding length is rather long. To optimize the resemblance to experiment, the theoretical spectrum in Fig. 2 is broadened with a Fano line shape. The strong Fano asymmetry ($q=6$) indicates strong autoionization.[45]

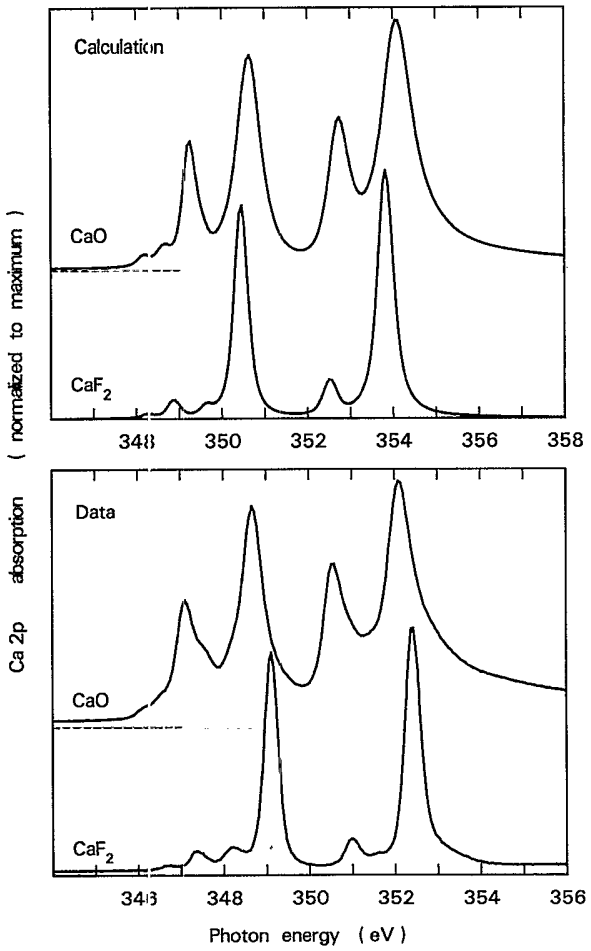

FIG. 1. Calculated and experimental Ca 2p absorption edges for Ca^{2+} in CaF_2 and CaO. The sign of the crystal-field parameter $10Dq$ reverses when going from the fluorite to the rocksalt structure ($10Dq=-0.75$ eV for CaF_2 and $10Dq=+1.2$ eV for CaO).

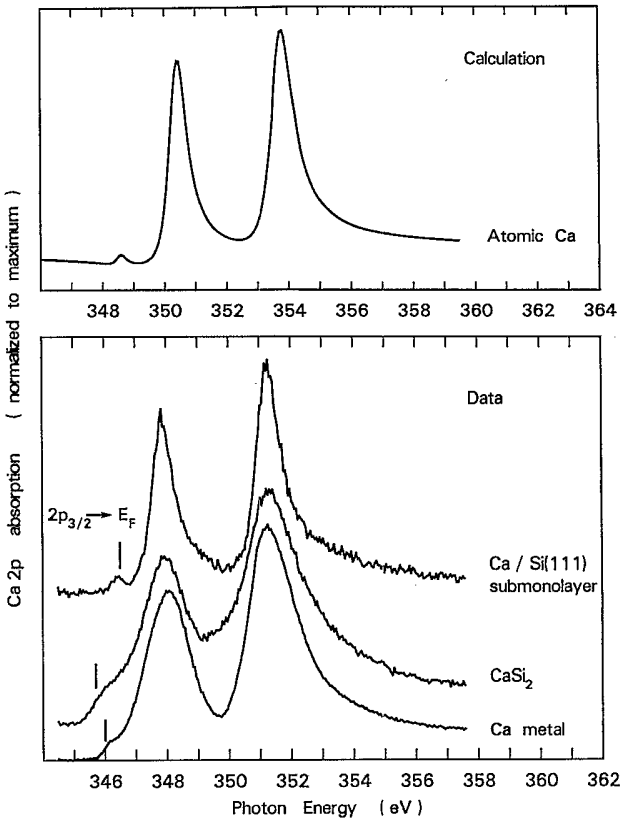

FIG. 2. Ca 2p absorption edges of Ca in metallic environments, i.e., Ca metal, $CaSi_2$, and a submonolayer of Ca on Si(111). The calculation represents a free atom without crystal field, with the broadening matched to the submonolayer case. The absorption edges in Ca metal and $CaSi_2$ exhibit the same three atomic lines, except broadened by band formation.

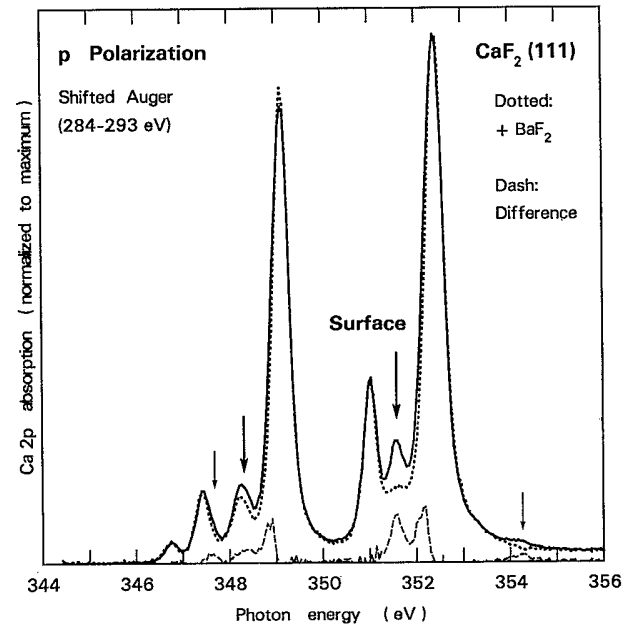

FIG. 3. Surface effects at the Ca 2p edge for clean $CaF_2(111)$. Surface-related features (arrows) are quenched by covering the surface with BaF_2, thereby creating a bulklike environment of the surface Ca atoms.

V. SURFACES AND INTERFACES

First, we will discuss surface effects, since they can be detected rather well. Interface features always show up together with surface features on thin film samples. To isolate them requires a good understanding of the surface contribution. The clean $CaF_2(111)$ surface exhibits several characteristic surface contributions to the Ca $2p$ edge, as indicated by arrows in Fig. 3 and in the experimental part of Fig. 4. Similar surface excitons have been observed for ionic[46–49] and rare gas[50,51] solids. The surface features on $CaF_2(111)$ are revealed by suppressing them with a few layers of adsorbed BaF_2 (overlapping dotted and solid curves in Figs. 3 and 4). BaF_2 exhibits the same ionic lattice as CaF_2 and thus provides a bulk-like environment for Ca surface atoms. The spectra in Fig. 3 are taken in the Auger detection mode with a probing depth of typically 20 Å, according to universal escape depth curves.[33] By moving the Auger detection window off the bulk Auger peak we have suppressed the two large bulk peaks in Fig. 3. The surface sensitivity can be further enhanced by detecting ions, emitted from the surface as decay product of the Ca $2p$ core holes. Low-energy ions do not penetrate more than one or two atomic layers.[41,52] Such spectra are shown in the experimental part of Fig. 4. As expected, the surface peaks are even stronger.

It is important to observe that the surface features depend on the polarization of the incident light (Fig. 4). Most of them are excited by the component of the electric-field vector perpendicular to the surface, which is present in p polarization only. In s polarization, on the

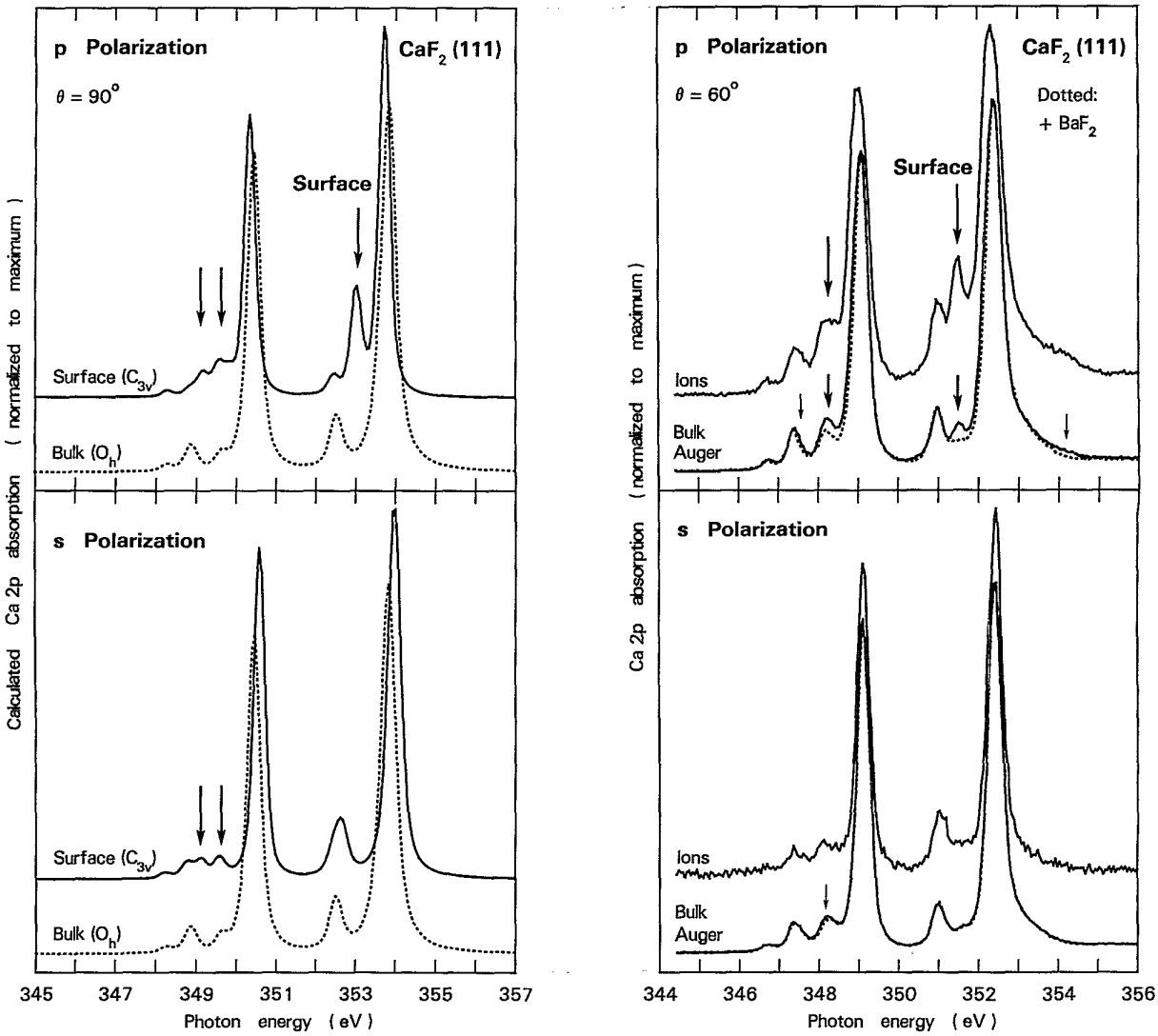

FIG. 4. Polarization dependence of surface features at the Ca $2p$ absorption edge of clean $CaF_2(111)$. (Calculated spectra on the left, experiment on the right.) The surface selectivity is enhanced experimentally by detecting photodesorbed (positive) ions instead of Auger electrons. Surface effects are quenched by covering the surface with BaF_2, as in Fig. 3. The most prominent surface feature at 351.5 eV is excited by the component of the electric-field vector perpendicular to the surface. The calculations explain the polarization dependence by the lower symmetry of the surface (C_{3v}) as opposed to the isotropic bulk (O_h).

other hand, the solid and dotted lines for the clean and BaF_2-covered surface nearly completely overlap each other, except for a region around 348 eV (bottom of the experimental part of Fig. 4). This strong polarization dependence of the surface features is in contrast to isotropic behavior of the bulk spectra, as represented by the BaF_2-covered surface.[53] No polarization dependence is expected from an isotropic bulk lattice, such as the cubic CaF_2 structure. The (111) surface, on the other hand, has a lower symmetry, giving rise to an anisotropy of the optical absorption. The F atom above the outermost Ca atom is missing, thereby lowering the symmetry to threefold C_{3v}. Consequently, the orbitals oriented perpendicular to the surface are not equivalent to orbitals oriented parallel to the surface. By using optical selection rules for the perpendicular component of the angular momentum m_j one can select orbitals of various orientations by using the orientation of the electric field vector. This prototype case shows that anisotropy could be useful for future, polarization-modulation experiments that separate surface and interface contributions from the bulk.

The extra peaks in the surface absorption spectrum and their polarization dependence can be calculated by taking into account the lowering of the symmetry from O_h for bulk Ca atoms to C_{3v} for surface Ca atoms, as shown in the theoretical part of Fig. 4. The parameters for the calculation are $10Dq = X^{400}U^{400} = -0.75$ eV, as in bulk CaF_2, $X^{4\bar{1}0} = -1.0$ eV, and $X^{2\bar{1}0} = +1.0$ eV. The extra surface features essentially originate from transitions that were symmetry forbidden in the bulk, but become allowed in the lower symmetry of the surface. The main surface feature at 351.5 eV is clearly accounted for, including its polarization dependence. Note that the experimental, p-polarized spectra include components of the electric-field vector parallel and perpendicular to the surface, since they are taken at angle of incidence of 60° from normal.[54] The other pair of extra surface features at lower energy (see arrows in the theoretical part of Fig. 4) has a counterpart in the difference spectra of Fig. 3 too, although less pronounced. Additional peaks in the difference spectra on the low-energy tail of the two big bulk lines are due to a narrowing of those lines upon BaF_2 adsorption. This may indicate an energy shift of the two principal lines from the bulk to the surface, as expected from the calculations. The pair of low-energy features is calculated to appear in s polarization as well as in p polarization. Comparing the clean and BaF_2-covered spectra for s polarization in Fig. 4 a slight, though inconclusive difference is seen near the calculated energy in s polarization (see fine arrow). Minor differences between calculation and experiment, e.g., a weak extra surface feature above 354 eV, could be due to the choice of the parameters for the surface crystal field, or due to the neglect of 4s final states.

An interface contribution to the Ca 2p absorption spectrum can be found at the CaF_2/Si(111) interface.[20,25,27] Figure 5 shows data for epitaxially grown CaF_2 films, normalized to the incident photon flux. Interface contributions can be identified by observing their attenuation when the film thickness is increased beyond a monolayer. Surface contributions, on the other hand, remain independent of thickness, while bulk contributions increase with thickness. Looking in Fig. 5 for spectral regions where the intensity (per incident photon) decreases with thickness, one finds two peaks at energies 0.6 eV below the two main bulk features. They are best seen in spectrum for two layers (solid line). For the five-layer film the interface peaks are attenuated, and a pair of surface features starts to dominate at an energy 0.3 eV below the interface structures (compare Figs. 3 and 4). In order to obtain the proper line shape for the interface layer we have tried to subtract the contribution of the outer layer from the two-layer spectrum by using the surface spectra from Fig. 4. This turned out to be difficult since small modifications of the sharp bulk lines have a large effect on the difference spectra. We have found that the best estimate of the interface spectrum is the monolayer spectrum, shown on a larger scale in Fig. 6. It is known from previous work[24–29] that both the Ca core-level shifts and the energy of the Ca-related interface state near the top of the valence band do not change when the first layer is covered by further layers. We can expect that the Ca 2p absorption spectra of the monolayer and the interface layer are similar, too. The monolayer spectrum in Fig. 6 depends on the polarization, reflecting a lowering of the

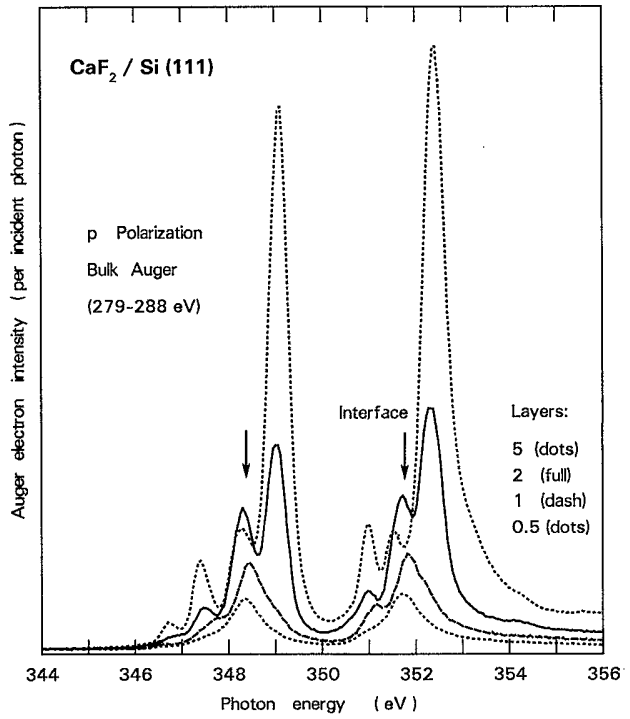

FIG. 5. Thickness dependence of the Ca 2p edge for CaF_2 grown epitaxially on Si(111). There is evidence for interface features from their attenuation with increasing film thickness (arrows). The interface signal is similar to that from the monolayer (dashed, for a closeup view see Fig. 6). Its two principal peaks are shifted down by 0.6 eV from the bulk.

symmetry to C_{3v}, analogous to that of the surface. This result suggests that polarization modulation techniques will be a useful tool for picking up the signal from buried interfaces.

For a theoretical analysis of the interface absorption we use the monolayer spectrum, as shown in Fig. 6. From its polarization dependence it is clear that the lowering of the symmetry to C_{3v} has to be taken into account. In addition, we will have to consider a possible valence change from Ca^{2+} to Ca^{1+}, as suggested previously.[20] The unpaired electron from the dangling bond at the Si(111) surface forces Ca into the 1+ oxidation state, such that it can form a bond using its unpaired 4*s* electron. In Fig. 7 we show the influence of a valence change on the theoretical spectrum (compare also the discussion in Sec. VI). The main effect is a shift to lower energy. This is also seen for the experimental spectra of the interface and the monolayer, supporting the view of a valence change from Ca^{2+} to Ca^{1+} at the CaF_2/Si(111) interface. Another effect is the generation of more lines: Whereas the $2p^6 3d^0 (J=0)$ to $2p^5 3d^1 (J=1)$ atomic multiplet has only three lines, the transition from $2p^6 3d^0 4s^1$ to $2p^5 3d^1 4s^1$ has eleven lines in the atomic case. The ground state now has $J=\frac{1}{2}$, because of the spin of the 4*s* electron. With the dipole selection rules the $J=\frac{1}{2}$ and $\frac{3}{2}$ final states can be reached, which are, respectively, fourfold and sevenfold degenerate. Projection to O_h symmetry causes a mixing of states and produces a total of 29 allowed transitions for a $J=\frac{1}{2}$ ground state, as can be inferred from the branching tables in Ref. 43. However, in Fig. 7 it can be seen that the effect on the spectral shape is minimal if the crystal field 10*Dq* is maintained at the bulk, CaF_2 value of -0.75 eV. Comparing the experimental spectrum of Fig. 6 with the calculations of Fig. 7, it is evident that the spectral shape is reproduced much better with a positive value of 10*Dq*, which is related to octahedral surroundings. This can be seen directly from the rather strong intensity of the extra peaks induced on the low-energy tails of the main doublet. They resemble those of CaO, which also has positive 10*Dq* (compare Fig. 1). The top spectrum in Fig. 7 gives the result for the Ca^{1+} $3d^0 4s^1$ state with $10Dq=+0.9$ eV. From the shift to lower energy and the close similarity to this octahedral simulation, we conclude that the interface spectrum is consistent with Ca^{1+} in a quasioctahedral surrounding. The polarization dependence shows that the symmetry is not exactly octahedral. This is because of the inequivalence of the surrounding Si and F atoms and their displacements from octahedral positions.

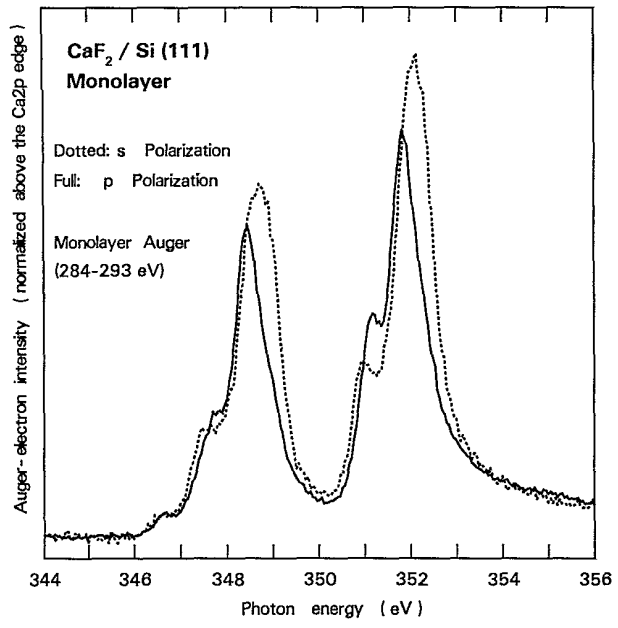

FIG. 6. Polarization-dependent Ca 2*p* absorption edges for a monolayer of CaF_2 on Si(111). These spectra are representative of the CaF_2/Si(111) interface as well. Figure 7 gives an approximate calculation, based on a valence change from Ca^{2+} to Ca^{1+} and a reversal of the crystal-field parameter 10*Dq*.

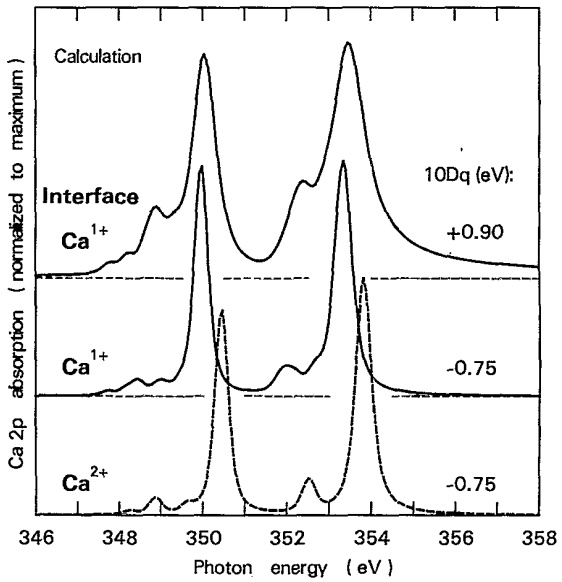

FIG. 7. Calculated Ca 2*p* edge fine structure for Ca^{2+} and Ca^{1+}, showing the effect of a valence change. The two bottom curves have a crystal field 10*Dq* corresponding to bulk CaF_2, the top curve has a crystal field with reverse sign, corresponding to the CaF_2/Si(111) interface. The multiplet structure of Ca^0 is similar to that of Ca^{2+} since the two configurations differ only by the filled Ca 4*s* shell.

VI. VALENCE DETERMINATION

In order to assess the effect of a valence change on the Ca 2*p* absorption spectrum experimentally, it is necessary to have reference compounds. Metallic Ca^0 and ionic Ca^{2+} compounds are readily available (see Sec. IV). They can be described by the same atomic multiplet structure (neglecting the perturbation by the crystal field), since they only differ by the filled Ca 4*s* shell. The Ca^{1+} configuration is unstable. The only reference that we have been able to find is provided by the *F* centers (Ca^{1+} ions next to an F vacancy) that are induced in Ca

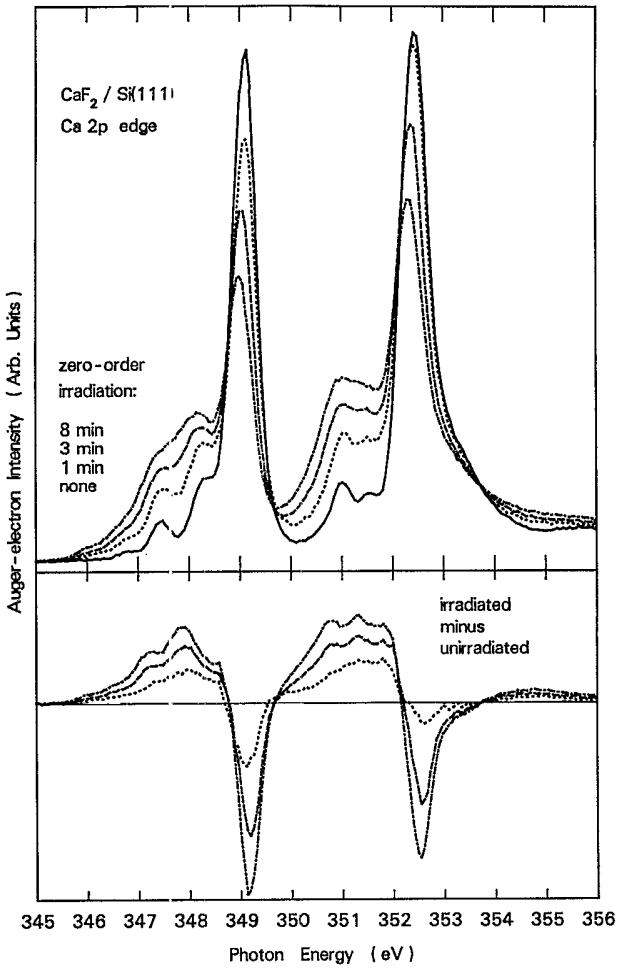

FIG. 8. Effect of soft x-ray irradiation on the Ca 2p edge of CaF_2. *F* centers are created at the surface (Ref. 40), which are used as representative of the Ca^{1+} valence state. The radiation dose is in the order of 10^{17} photons/cm^2.

halides by irradiation with electrons or photons. For the $CaF_2(111)$ surface it has been found that an ordered monolayer of surface F centers can be formed.[40] Figure 8 shows Ca 2p absorption spectra for radiation doses in the appropriate range.[55] The main effect of irradiation is a shift of spectral weight from the main two peaks down to a broad feature at about 1.2 eV lower energy. Some fine structure appearing in the difference spectra is caused by a broadening of the spectral features of CaF_2. The downwards shift can be rationalized by noticing that the extra Ca 4s electron induces a Ca 2p core-level shift towards lower binding energy (about 3.8 eV). Note that the core-level shift is smaller than that of the absorption edge. This is also true for the CaF_2/Si(111) interface where the shift is 2.1 eV for the Ca 2p core level[27] and 0.6 eV for the Ca 2p absorption peaks. The difference between the core-level and the absorption edge shifts is due to the fact that the excited Ca 3d electron in the Ca 2p-to-3d absorption process resides partly inside the charge distribution of the Ca 4s electron, i.e., the 2p and the 3d states both experience a shift in the same direction. Therefore the shifts of the upper and lower state partially compensate each other in the absorption process. The theoretical prediction for the effect of a valence change from Ca^{2+} to Ca^{1+} has already been discussed with Fig. 7. The main feature is a shift towards lower energy, as observed experimentally.

VII. SUMMARY

The Ca 2p-to-3d absorption edge is found to exhibit a variety of multiplet structures for bulk compounds, surfaces, and interfaces. In the bulk, the fine structure develops from an atomiclike triplet for metallic compounds to a seven-line multiplet for ionic compounds. The latter is produced by the splitting of the 3d orbitals in a strong crystal field. The sign of the crystal field can be reversed by varying the crystal structure from rocksalt (with octahedral coordination) to fluorite (with cubic coordination). At surfaces, extra multiplet lines show up due to the lower symmetry. They become polarization dependent, as opposed to the isotropic bulk lines. The same phenomena are observed at interfaces, thereby opening up the possibility of applying polarization modulation techniques in order to selectively observe surface or interface absorption. A change of valence from Ca^{2+} to Ca^{1+} is calculated to shift the main absorption lines down in energy, in agreement with results from *F* centers in CaF_2. Such a shift is also observed at the CaF_2/Si(111) interface, indicating a valence change from Ca^{2+} to Ca^{1+}.

This type of analysis can be extended to a variety of other materials, i.e., using atomic-multiplet plus crystal-field effects to distinguish the atomic environment. In general, one needs an absorption edge with sufficiently localized character. While it is too early to say definitively for how many elements the present approach would be appropriate, it certainly is appropriate for K, Ca, and the 3d transition metal series, using the 2p absorption edge. In addition, there are strong indications that a similar approach, combined with the use of polarized light and single-crystal samples, will be a source of information for the lanthanides, using the 3d and 4d edges. We also have some indication that the approach may work for the 2p edges of the 4d transition metal series, but here, and for other elements like the 3d and 4d edges of actinides, more work is needed to define the situation clearly.

ACKNOWLEDGMENTS

This research was carried out (in part) at the National Synchrotron Light Source, Brookhaven National Laboratory, which is supported by the U.S. Department of Energy, Division of Materials Sciences and Division of Chemical Sciences.

*Present address: Max-Lab, University of Lund, Box 118, S-22100, Lund, Sweden.
†Present address: Department of Physics, Queen's University, Kingston, Ontario, Canada K7L 3N6.

[1]J. Stohr and D. A. Outka, J. Vac. Sci. Technol. A **5**, 919 (1987).
[2]G. Kaindl, G. Kalkowski, W. D. Brewer, B. Perscheid, and F. Holtzberg, J. Appl. Phys. **55**, 1910 (1984).
[3]B. T. Thole, G. van der Laan, J. C. Fuggle, G. A. Sawatzky, R. C. Karnatak, and M.-M. Esteva, Phys. Rev. B **32**, 5107 (1985).
[4]R. D. Leapman, L. A. Grunes, and P. L. Fejes, Phys. Rev. B **26**, 614 (1982).
[5]J. E. Müller, O. Jepsen, and J. W. Wilkins, Solid State Commun. **42**, 365 (1982).
[6]T. Yamaguchi, S. Shibuya, S. Suga, and S. Shin, J. Phys. C **15**, 2641 (1982).
[7]J. Barth, F. Gerken, and C. Kunz, Phys. Rev. B **28**, 3608 (1983).
[8]J. Fink, Th. Müller-Heinzerling, B. Scheerer, W. Speier, F. U. Hillebrecht, J. C. Fuggle, J. Zaanen, and G. A. Sawatzky, Phys. Rev. B **32**, 4899 (1985).
[9]J. Zaanen, G. A. Sawatzky, J. Fink, W. Speier, and J. C. Fuggle, Phys. Rev. B **32**, 4905 (1985).
[10]E. E. Koch, Y. Jugnet, and F. J. Himpsel, Chem. Phys. Lett. **116**, 7 (1985).
[11]G. van der Laan, B. T. Thole, G. A. Sawatzky, and M. Verdaguer, Phys. Rev. B **37**, 6587 (1988).
[12]F. M. F. de Groot, J. C. Fuggle, B. T. Thole, and G. A. Sawatzky, Phys. Rev. B **41**, 928 (1990).
[13]F. Sette, B. Sinkovic, Y. J. Ma, and C. T. Chen, Phys. Rev. B **39**, 11 125 (1989).
[14]C. T. Chen and F. Sette, Phys. Scr. **T31**, 119 (1990).
[15]F. M. F. de Groot, J. C. Fuggle, B. T. Thole, and G. A. Sawatzky, Phys. Rev. B **42**, 5459 (1990).
[16]D. D. Sarma, O. Strebel, C. T. Simmons, U. Neukirch, G. Kaindl, R. Hoppe, and H. P. Müller, Phys. Rev. B **37**, 9784 (1988).
[17]A. Bianconi, M. De Santis, A. DiCicco, A. M. Flank, A. Fontaine, P. Lagarde, H. Katayama-Yoshida, A. Kotani, and Marcelli, Phys. Rev. B **38**, 7196 (1988).
[18]M. Grioni, J. B. Goedkoop, R. Schoorl, F. M. F de Groot, J. C. Fuggle, F. Schäfers, E. E. Koch, G. Rossi, J.-M. Esteva, and R. C. Karnatak, Phys. Rev. B **39**, 1541 (1989).
[19]K. Okada and A. Kotani, J. Phys. Soc. Jpn. **58**, 1095 (1989).
[20]F. J. Himpsel, U. O. Karlsson, J. F. Morar, D. Rieger, and J. A. Yarmoff, Phys. Rev. Lett. **56**, 1497 (1986); see also C. T. Chen and F. Sette, *ibid.* **60**, 160 (1988); and F. J. Himpsel, U. O. Karlsson, J. F. Morar, D. Rieger, and J. A. Yarmoff, *ibid.* **60**, 161 (1988).
[21]M. W. D. Mansfield, Proc. R. Soc. London Ser. A **348**, 143 (1976).
[22]A. A. Maiste, R. E. Ruus, and M. A. Elango, Zh. Eksp. Teor. Fiz. **79**, 1671 (1980) [Sov. Phys.—JETP **52**, 844 (1980)].
[23]J. M. Kenney, C. Jacobsen, J. Kirz, H. Rarback, F. Cinotti, W. Thomlinson, R. Rosser, and G. Schidlowsky, J. Microscopy **138**, 321 (1985).
[24]F. J. Himpsel, F. U. Hillebrecht, G. Hughes, J. L. Jordan, U. O. Karlsson, F. R. McFeely, J. F. Morar, and D. Rieger, Appl. Phys. Lett. **48**, 596 (1986).
[25]U. O. Karlsson, F. J. Himpsel, J. F. Morar, D. Rieger, and J. A. Yarmoff, J. Vac. Sci. Technol. B **4**, 1117 (1986).
[26]M. A. Olmstead, R. I. G. Uhrberg, R. D. Bringans, and R. Z. Bachrach, J. Vac. Sci. Technol. B **4**, 1123 (1986).
[27]D. Rieger, F. J. Himpsel, U. O. Karlsson, F. R. McFeely, J. F. Morar, and J. A. Yarmoff, Phys. Rev. B **34**, 7295 (1986).
[28]M. A. Olmstead, R. I. G. Uhrberg, R. D. Bringans, and R. Z. Bachrach, Phys. Rev. B **35**, 7526 (1987).
[29]A. B. McLean and F. J. Himpsel, Phys. Rev. B **39**, 1457 (1989).
[30]T. F. Heinz, F. J. Himpsel, E. Palange, and E. Burstein, Phys. Rev. Lett. **63**, 644 (1989).
[31]F. J. Himpsel, Y. Jugnet, D. E. Eastman, J. J. Donelon, D. Grimm, G. Landgren, A. Marx, J. F. Morar, C. Oden, R. A. Pollak, J. Schneir, and C. A. Crider, Nucl. Instrum. Methods **222**, 107 (1984).
[32]D. E. Eastman, J. J. Donelon, N. C. Hien, and F. J. Himpsel, Nucl. Instrum. Methods **172**, 327 (1980).
[33]We also used secondary electron detection (not shown) and obtained results similar to the Auger detection mode, nearly independent of the kinetic energy of the secondary electrons. The surface sensitivity did not increase significantly near the escape depth minimum of the secondary electrons. This is probably due to the fact that most of the secondary electrons originate from Ca 2*p* Auger electrons near the Ca 2*p* threshold, and therefore have an escape depth equal to that of the Auger electrons plus that of the secondary electrons.
[34]M. Meyer, E. v. Raven, M. Richter, B. Sonntag, R. D. Cowan, and J. E. Hansen, Phys. Rev. A **39**, 4319 (1989).
[35]T. Tiedje, K. M. Colbow, D. Rogers, and W. Eberhardt, Phys. Rev. Lett. **65**, 1243 (1990).
[36]F. M. F. De Groot *et al.* (unpublished).
[37]W. Gudat and C. Kunz, Phys. Rev. Lett. **29**, 169 (1972).
[38]CaO single crystals were obtained from W. C. Spicer Ltd., 1276 Vanbrugh Hill, Greenwich, London SE 10, UK.
[39]J. F. Morar and M. Wittmer, J. Vac. Sci. Technol. A **6**, 1340 (1988).
[40]U. O. Karlsson, F. J. Himpsel, J. F. Morar, F. R. McFeely, D. Rieger, and J. A. Yarmoff, Phys. Rev. Lett. **57**, 1247 (1986).
[41]R. Souda and M. Aono, in *The Structure of Surfaces II,* edited by J. F. van der Veen and M. A. van Hove, Springer Series in Surface Science Vol. 11 (Springer-Verlag, Berlin, 1987), p. 581.
[42]F. Senf, thesis, Hamburg, 1987 (unpublished).
[43]P. H. Butler, *Point Group Symmetry, Applications, Methods and Tables* (Plenum, New York, 1981).
[44]B. T. Thole (unpublished).
[45]U. Fano, Phys. Rev. **124**, 1866 (1961).
[46]V. E. Henrich, G. Dresselhaus, and H. J. Zeiger, Phys. Rev. Lett. **36**, 158 (1976).
[47]Y. Rehder, W. Gudat, R. G. Hayes, and C. Kunz, in *Proceedings of the Seventh International Vacuum Congress and Third Conference of Solid Surfaces,* edited by R. Dobrozemsky, F. Rüdenauer, F. P. Viehböck, and A. Breth (IVC, ICSS, Wien, 1977), p. 453.
[48]O. Aita, K. Ichikawa, and K. Tsutsumi, Phys. Rev. B **38**, 10079 (1988).
[49]K. Ichikawa, O. Aita, and K. Tsutsumi, Phys. Rev. B **39**, 1307 (1989)
[50]V. Saile, M. Skibowski, W. Steinmann, P. Gürtler, E. E. Koch, and A. Kozevnikov, Phys. Rev. Lett. **37**, 305 (1976).
[51]V. Saile and E. E. Koch, Phys. Rev. B **20**, 784 (1979).
[52]E. Taglauer and W. Heiland, Appl. Phys. **9**, 261 (1976).
[53]A slight remnant of the upper surface peak is seen in the spectra of the BaF_2-covered surface for *p* polarization. This could be due to incomplete BaF_2 coverage, e.g., caused by island formation.
[54]The ion spectrum appears to contain some extra bulk contribution, even taking the mixture of parallel and perpendicular

components in p polarization at $\theta=60°$ into account. This might be explained by the open structure of the $CaF_2(111)$ surface, where F above the second layer Ca can be emitted into vacuum without colliding with other atoms.

[55]For the higher radiation doses a further conversion of Ca^{1+} to metallic Ca^0 is beginning to take place. This may explain that the energy shift is larger than at the CaF_2/Si(111) interface.